JACS
JOURNAL OF THE AMERICAN CHEMICAL SOCIETY
Article
pubs.acs.org/JACS

Prediction of Remarkable Ambipolar Charge-Transport Characteristics in Organic Mixed-Stack Charge-Transfer Crystals

Lingyun Zhu, Yuanping Yi, Yuan Li, Eung-Gun Kim,† Veaceslav Coropceanu,* and Jean-Luc Brédas*,‡

School of Chemistry and Biochemistry and Center for Organic Photonics and Electronics, Georgia Institute of Technology, Atlanta, Georgia 30332-0400, United States

Supporting Information

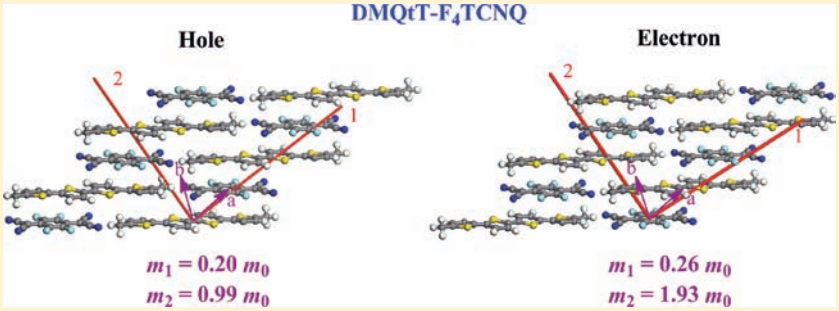

ABSTRACT: We have used density functional theory calculations and mixed quantum/classical dynamics simulations to study the electronic structure and charge-transport properties of three representative mixed-stack charge-transfer crystals, DBTTF−TCNQ, DMQtT−F_4TCNQ, and STB−F_4TCNQ. The compounds are characterized by very small effective masses and modest electron−phonon couplings for both holes and electrons. The hole and electron transport characteristics are found to be very similar along the stacking directions; for example, in the DMQtT−F_4TCNQ crystal, the hole and electron effective masses are as small as 0.20 and 0.26 m_0, respectively. This similarity arises from the fact that the electronic couplings of both hole and electron are controlled by the same superexchange mechanism. Remarkable ambipolar charge-transport properties are predicted for all three crystals. Our calculations thus provide strong indications that mixed-stack donor−acceptor materials represent a class of systems with high potential in organic electronics.

1. INTRODUCTION

Organic semiconductors have attracted much attention in recent years as they combine the electrical and optical properties typical of inorganic semiconductors with properties such as flexibility, low cost, and structural tunability via chemical modification.[1] In particular, oligoacenes such as pentacene and rubrene have triggered significant interest as active components in (opto)electronic devices because of their high charge carrier mobilities.[2] Still, shortcomings such as poor solubility or limited stability have weakened the viability of oligoacene-based devices, and many efforts are made to design new molecular systems with improved performance. Up to now, most of these efforts have dealt, however, with semiconductors based on a *single* component (organic molecule) building block. Intriguingly, it has been recently suggested that multicomponent organic systems, in particular binary charge-transfer (CT) compounds composed of two types of molecules where one molecule acts as a donor (D) and the other as an acceptor (A), could open new opportunities for organic electronics.[3−5]

The most famous representative of an organic conducting CT system is tetrathiafulvalene−7,7,8,8-tetracyanoquinodimethane (TTF−TCNQ).[6] Since the discovery of metallic conductivity in TTF−TCNQ[6,7] and superconductivity in $(TMTSF)_2PF_6$ (TMTSF = tetramethyltetraselenafulvalene),[8] CT systems have received significant theoretical and experimental attention.[9,10] However, the bulk of these studies was mainly devoted to a basic understanding of their unconventional (super)conducting, magnetic, and other properties.[3,5,9,10] Only more recently were CT systems considered for application in organic electronics.[3−5,11] It was shown, for instance, that field-effect transistors (FETs) based on (BEDT−TTF)(F_2TCNQ) (BEDT = bis(ethylenedithio)-tetrathiafulvalene, F_2TCNQ = 2,5-difluorotetracyanoquinodimethane)[12] or (BEDT−TTF)(TCNQ)[13] as active element exhibit ambipolar characteristics. Also, it was reported that metallic CT compounds can be used as source/drain electrodes to improve charge injection;[14] organic FETs using crystalline DBTTF−TCNQ (DBTTF = dibenzotetrathiafulvalene) as channel and TTF−TCNQ as source and drain electrodes were shown to outperform similar devices with Au and Ag electrodes.[14,15]

Binary CT compounds with 1:1 stoichiometry can be divided into two groups according to their crystal structure, either segregated-stack or mixed-stack systems. In the former case, a

Received: November 1, 2011
Published: January 3, 2012

   dx.doi.org/10.1021/ja210284s | J. Am. Chem.Soc. 2012, 134, 2340−2347

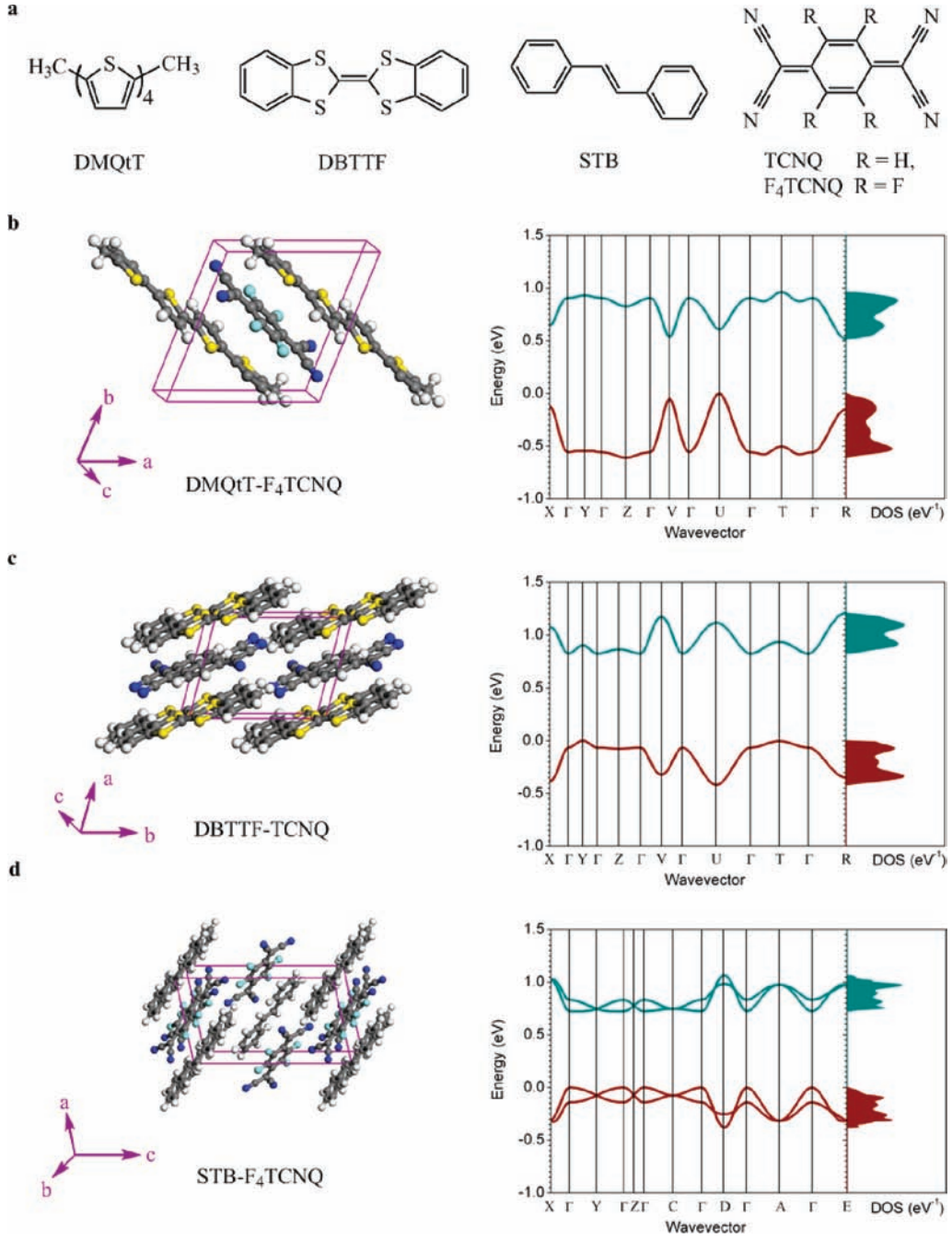

Figure 1. Chemical, crystal, and band structures of the investigated systems: (a) chemical structures; (b–d) crystal and band structures. The cell parameters are as follows: DBTTF–TCNQ (a = 9.215 Å, b = 10.644 Å, c = 7.734 Å, α = 113.32°, β = 122.28°, and γ = 67.66°), DMQtT–F_4TCNQ (a = 10.185 Å, b = 10.568 Å, c = 6.482 Å, α = 98.92°, β = 95.89°, and γ = 67.24°), and STB–F_4TCNQ (a = 9.555 Å, b = 6.287 Å, c = 17.295 Å, α = 90.00°, β = 99.99°, and γ = 90.00°). The points of high symmetry in the first Brillouin zone are labeled as follows: Γ = (0, 0, 0); X = (0.5, 0, 0); Y = (0, 0.5, 0); Z = (0, 0, 0.5); V, A = (0.5, 0.5, 0); U, D = (0.5, 0, 0.5); T, C = (0, 0.5, 0.5), and R, E = (0.5, 0.5, 0.5), all in crystallographic coordinates. The zero of energy is given at the top of the valence band.

classical example being TTF–TCNQ, the donor and acceptor molecules form adjacent separated (...–A–A–A–... and ...–D–D–D–...) stacks;[16] when free of Peierls, charge-order, or other instabilities, these systems display high electrical conductivity along the stacking directions and even metallic behavior at room temperature.[17−19] In mixed-stack systems, the donor and acceptor molecules alternate along the stacking (...–D–A–D–A–...) directions; this is the case, for instance, for acene (antracene,[20] naphthalene,[21] tetracene,[22,23] and perylene[22,24])–TCNQ crystals and compounds formed by combining TTF derivatives with TCNQ or F_4TCNQ (F_4TCNQ = 2,3,5,6-tetrafluoro-7,7,8,8-tetracyanoquinodimethane).[25−27] Under ambient conditions, mixed-stack systems are as a rule semiconductors or insulators.

We have investigated the electronic structure and charge-transport parameters of a series of CT systems. In this contribution, we have chosen to focus on three representative mixed-stack CT crystals, DBTTF–TCNQ, DMQtT–F_4TCNQ (DMQtT = dimethylquaterthiophene), and STB–F_4TCNQ (STB = stilbene), see Figure 1, that allow us to rationalize the

dx.doi.org/10.1021/ja210284s | J. Am. Chem.Soc. 2012, 134, 2340–2347

charge-transport properties of mixed-stack CT crystals and discuss their potential for organic electronics.

2. METHODOLOGY

The geometry optimizations of the crystal structures were performed using density functional theory with the 6-31G basis set and the B3LYP functional. During optimization, the positions of the atoms in the unit cell were relaxed while the cell parameters were kept fixed at the experimental values. Uniform 8 × 6 × 8, 6 × 6 × 8, and 6 × 8 × 4 Monkhorst−Pack k-point mesh were employed for the DBTTF−TCNQ, DMQtT−F_4TCNQ, and STB−F_4TCNQ crystals, respectively. The electronic band structures and densities of states (DOS) were calculated at the 6-31G/B3LYP and 6-31G/BHandHLYP levels of theory, using the optimized crystal structures. The inverse effective mass tensor for the three-dimensional crystal, m_{ji}^{-1}, is defined as

$$\frac{1}{m_{ij}} = \frac{1}{\hbar^2}\frac{\partial^2 E}{\partial k_j \partial k_i} \quad (1)$$

where subscripts i and j denote the Cartesian coordinates in reciprocal space, E the band energy, $\hbar$ the Planck constant, and k the electron wave vector. Subsequent diagonalization of m_{ji}^{-1} provides the principal components and their orientations. The inverse effective mass tensor was calculated by means of Sperling's centered difference method with dk = 0.01/bohr. The Γ-point lattice phonons were derived by means of numerical differentiation using a 0.003 Å atomic displacement step. All crystal band-structure and normal-mode calculations were carried out using the CRYSTAL06 package.[28]

The effective transfer integrals for nearest-neighbor pairs of donor−acceptor molecules at the optimized crystal geometry were evaluated by using a fragment orbital approach in combination with a basis set orthogonalization procedure.[29] These calculations were performed with the 6-31G (d,p) basis set and using the B3LYP, BHandHLYP, and (long-range corrected) ωB97X functionals (see Supporting Information for more details). The calculations of the transfer integrals were carried out with the Gaussian 03 package.[30]

3. RESULTS AND DISCUSSION

3.1. Crystal Structure. The crystalline structures of DBTTF−TCNQ[27] and DMQtT−F_4TCNQ[31] belong to the triclinic space group $P\bar{1}$, while the crystalline structure of STB−F_4TCNQ[32] to the $P2_1/n$ monoclinic space group (see Figure 1). The three systems have 1:1 stoichiometry and crystallize in mixed-stack arrays along the a-axis. The calculated electronic band structures are given in Figure 1. In all crystals, the wave functions of the valence bands (VBs) are dominated by the highest occupied molecular orbitals (HOMOs) of the donor molecules and the wave functions of the conduction bands (CBs) by the lowest unoccupied molecular orbitals (LUMOs) of the acceptor molecules. Since the DBTTF−TCNQ and DMQtT−F_4TCNQ crystals contain one donor and one acceptor molecule per unit cell, their valence and conduction bands display a simple motif. In contrast, STB−F_4TCNQ contains two translationally inequivalent donor and acceptor molecules per unit cell; as a result, their CBs and VBs present a two-subband structure. The VB and CB widths are relatively large, in the range of 380−610 and 340−450 meV, respectively (see Table S1 in the Supporting Information), with DMQtT−F_4TCNQ displaying the largest widths for both VB and CB (610 and 450 meV, respectively). In all cases the largest VB and CB dispersions occur along the stacking directions. However, in nearly all cases, the bandwidth along this direction is substantially smaller than the total bandwidth, which suggests that there exist significant electronic couplings along other directions as well. The derived bandwidths are comparable to those computed for the pentacene crystal[33,34] (610 and 590 meV for VB and CB, respectively) and nearly twice as large as those in rubrene[35] (340 and 160 meV for VB and CB, respectively).

A remarkable electronic feature, which is especially apparent along the stacking direction, is the quasi mirror symmetry between the CBs and VBs (see Figure 1). This result suggests that the electronic interactions (transfer integrals) for holes and electrons are very similar. At this stage, it is important to underline that, in contrast to typical one-component organic semiconductors such as oligoacenes where charge transport is defined by the transfer integrals between neighboring molecules[34] (we denote these transfer integrals as t^{direct}), the situation is more complex in CT systems. Indeed, along the stacking directions where the VBs and CBs display the largest bandwidths, the direct wave function overlap between the closest donor molecules (or between the closest acceptor molecules) is zero. Actually, the electronic couplings found here have a superexchange nature; i.e., the electronic coupling for holes results from the mixing of the frontier orbitals of two closest donor molecules with the orbitals of the "bridging" acceptor molecule and vice versa for electrons. Generally speaking, the transfer integrals can contain contributions both from direct (through-space) interactions and from a superexchange mechanism (we refer to those here as effective transfer integrals, t^{eff}).

The electronic-structure calculations reveal that, in all three crystals, the electronic couplings, $t_{H_D-L_A}$, between the HOMO of a donor and the LUMO of the adjacent acceptor along the stacking direction are in the range of 300−500 meV (see Table S2 in the Supporting Information). Using perturbation theory and assuming that only this pathway contributes to the superexchange mechanism, we obtain that the effective transfer integrals for holes and electrons along the stacking directions are equal and are given by

$$t^{\text{eff}}_{H_D-H_D} = t^{\text{eff}}_{L_A-L_A} = \frac{t^2_{H_D-L_A}}{\Delta E} \quad (2)$$

Here, $\Delta E = E(D^1A^{-1}) - E(D^0A^0)$ represents the energy of the CT state of the DA dyad. This result implies that, when the electronic coupling is dominated by such a superexchange mechanism, a mirror symmetry between the VB and CB should be expected. Importantly, this is the case for the three systems investigated here. We note, however, that previous electronic-structure calculations for tetracene−TCNQ[22] and preliminary results we have obtained for some other mixed-stack compounds indicate that in some instances the superexchange coupling can be comparable to, or even smaller than, the contributions from direct D−D and A−A interactions; in such cases, no electron−hole symmetry is observed.

We note that since eq 2 is based on perturbation theory, it can only provide a crude estimate of the transfer integrals. In order to gain a more accurate evaluation, we have used an energy-splitting approach. In contrast to the usual situation for through-space interactions between two adjacent molecules where the transfer integrals can be derived from the molecular

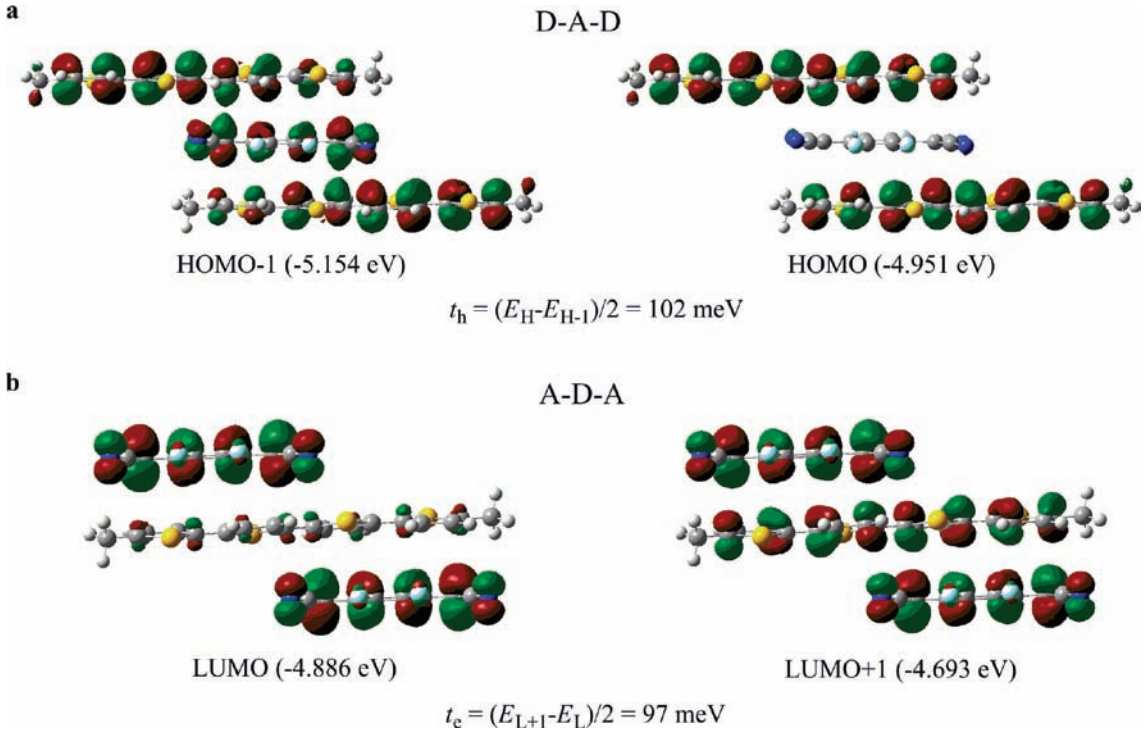

Figure 2. Energy-splitting estimates of the transfer integrals along the stacking direction in the DMQtT−F_4TCNQ crystal: (a) holes and (b) electrons.

energy levels of the corresponding dimer,[29,34] here it is necessary to use the energy levels of a molecular cluster. The approach used to compute the effective transfer integrals along the stacking directions is illustrated in Figure 2. The computed transfer integrals and the crystal directions along which these integrals possess the largest values are shown in Figure 3. In agreement with the band-structure results, the estimated transfer integrals are large for both holes, 51−102 meV, and electrons, 45−97 meV (we note that, in a simple one-dimensional tight-binding approximation, the bandwidths correspond to four times the transfer integrals). For each system, the transfer integrals for holes and electrons are very similar, in agreement with eq 2. The largest transfer integrals are obtained for DMQtT−F_4TCNQ, 102 and 97 meV for holes and electrons, respectively. These results are consistent with the fact that the degree of charge-transfer, or ionicity parameter $\delta(D^{\delta+}A^{\delta-})$, obtained from a simple Mulliken population analysis is also larger in DMQtT−F_4TCNQ, $\delta \sim 0.3$, than in the other two systems, for which $\delta \sim 0.1$. For the sake of comparison, we recall that the largest transfer integrals in pentacene (for both holes and electrons) are smaller, on the order of 85 meV.[36] Thus, the calculations show that, in spite of their superexchange nature, *the transfer integrals in CT crystals can be as large as or even larger than in the best single-component organic semiconductors*.

As a consequence of the large transfer integrals and bandwidths, the effective masses along the stacking direction (this component is labeled as m_1, see Figure 3) are very small, in the range of 0.2−0.46 m_0 (m_0 is the electron mass in vacuum) for holes and 0.26−0.48 m_0 for electrons. Remarkably small effective masses for both holes (0.2 m_0) and electrons (0.26 m_0) are found in DMQtT−F_4TCNQ. In agreement with the results of the band-structure calculations discussed above, the effective mass tensor presents an additional (m_2) small component (<2.30 m_0) along a direction nearly perpendicular to the molecular stacks (see Figure 3). For instance, the m_2 values for holes and electrons in DMQtT−F_4TCNQ are about 0.99 and 1.93 m_0, respectively. This finding suggests that, while charge transport is most favorable along the stacking direction, it can exhibit some useful two-dimensional character. Interestingly, although the electronic couplings in our CT systems and in oligoacenes are comparable, the effective masses are much smaller in the former (the smallest effective mass component for holes is about 1.7 m_0 in pentacene[37] and 0.94 m_0 in rubrene[38]). This result can be explained by the fact that the effective mass also depends on the effective hopping distance ($m = \hbar^2/2td^2$, d = distance); this distance along the stacking direction in the CT systems is much larger than (basically at least twice as large as) the characteristic distances between adjacent strongly interacting molecules in oligoacene crystals.

3.2. Electron−Vibration Coupling. In addition to electronic interactions, the charge-transport properties also depend on electron−phonon interactions. As discussed in detail elsewhere, in organic semiconductors, there exist two major electron−phonon (vibration) coupling mechanisms.[16,34] The first is referred to as local coupling and arises from the modulation of the site energy by vibrations; it represents the key interaction considered in conventional electron-transfer theory and in Holstein's molecular polaron model.[39,40] The second mechanism is referred to as nonlocal coupling and comes from the modulation of the transfer integrals by vibrations (Peierls-type coupling).[41]

The overall strength of the local coupling is usually expressed via the polaron binding energy E_{pol} or, in the context of electron-transfer theory, by the reorganization energy λ ($\approx 2E_{pol}$).[34] It consists of both intra- and intermolecular contributions; the former reflects the changes in the geometry

dx.doi.org/10.1021/ja210284s | J. Am. Chem.Soc. 2012, 134, 2340−2347

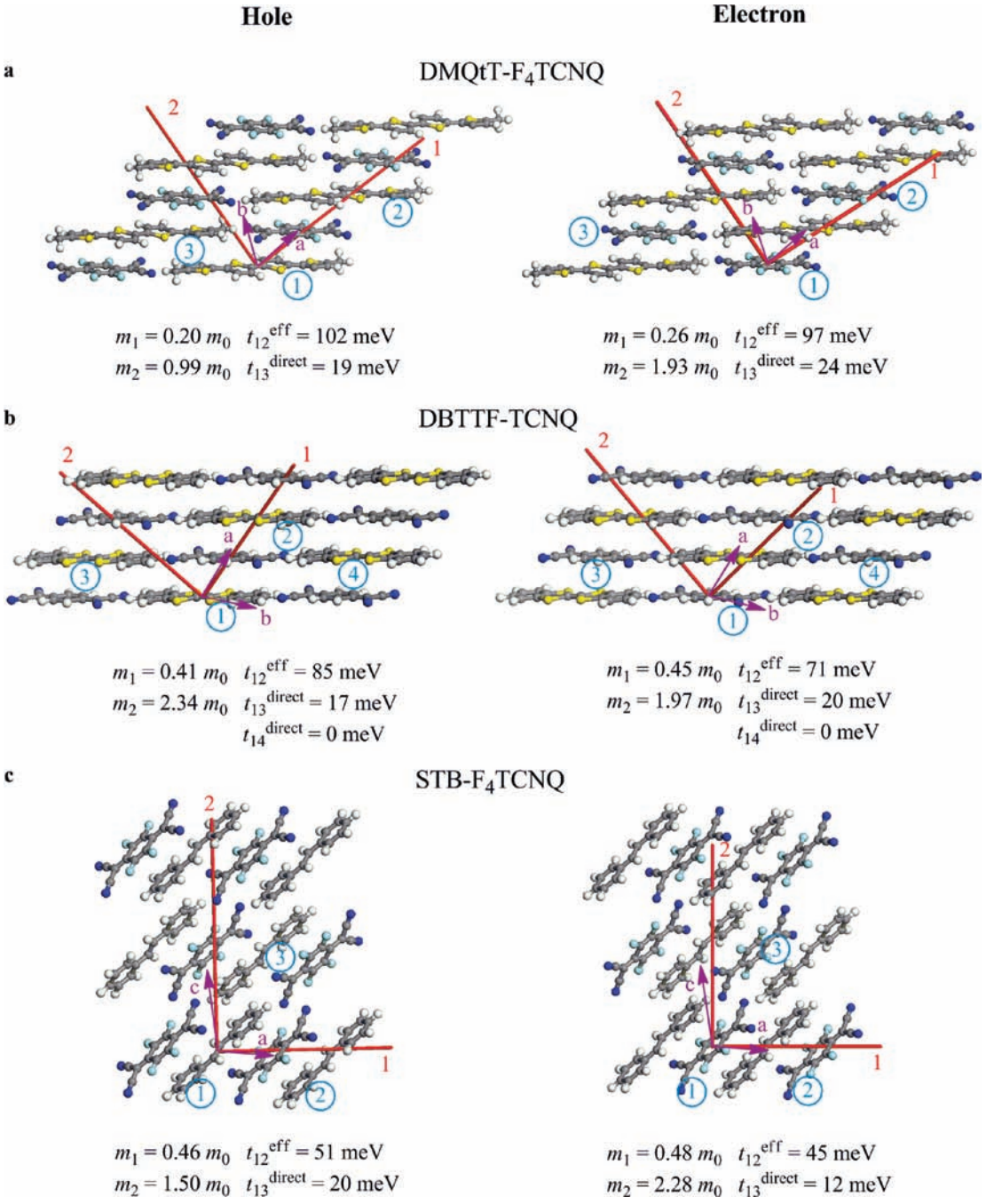

Figure 3. Illustration of the most important charge-transport pathways for holes and electrons. The red lines indicate the directions along which the principal components of m_{ji}^{-1} have the smallest values for the effective mass values.

of individual molecules and the latter in the polarization of the surrounding molecules, upon going from the neutral to the charged state and vice versa. It has been shown[34,42,43] that, in the systems such as oligoacenes, the intermolecular contribution to E_{pol} is substantially smaller than the intramolecular component. We therefore focus here first on the Holstein type of local electron−phonon coupling due to intramolecular vibrations. We stress, however, that due to some ionic character (partial charge transfer in the ground state) the intermolecular contribution in the present systems might be at some extent larger than in oligoacenes. We recall that the polaron binding energy for electrons is related to the geometry relaxations taking place upon adding one electron to the acceptor unit, i.e., either F_4TCNQ or TCNQ. The computed E_{pol} values for both acceptors are nearly equal, 129 and 128 meV for F_4TCNQ and TCNQ, respectively. These values are about twice as large as in pentacene[44] (66 meV) but comparable to that in rubrene[35,45] (96 meV). The contributions to the polaron binding energies from the various vibration modes are shown in Figure 4. As seen from Figure 4b the electrons mostly interact with high-frequency vibration modes. In the case of DBTTF and DMQtT, the gas-phase DFT calculations predict a twisted geometry for the neutral state and a planar geometry for the cation state. Therefore, the holes in these systems are also coupled to the low-frequency vibrations (see Figure 4a). However, since in the solid state these molecules tend toward a

dx.doi.org/10.1021/ja210284s | J. Am. Chem.Soc. 2012, 134, 2340−2347

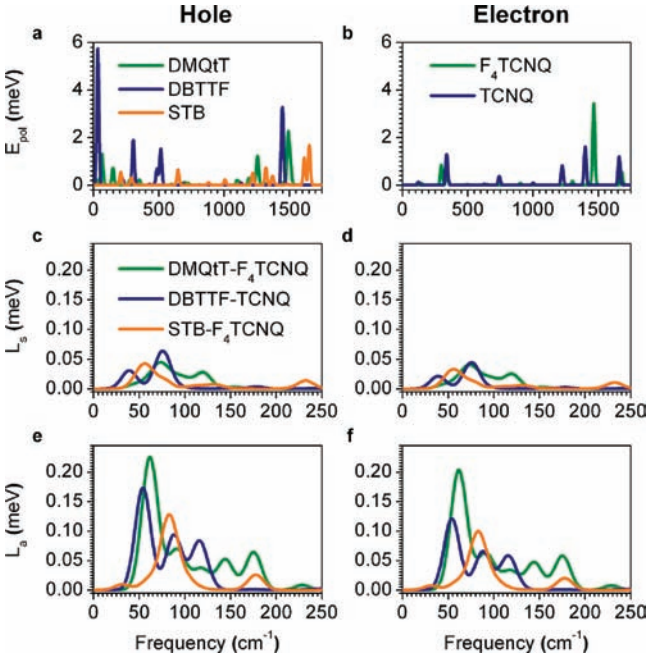

Figure 4. Spectra of polaron binding energies E_{pol} and parameter L. Polaron binding energies: (a) for the cations of DMQtT, DBTTF, and STB and (b) for the anions of F_4TCNQ and TCNQ. Parameter L for hole and electron for symmetric (c, d) and antisymmetric (e, f) normal modes in the DMQtT−F_4TCNQ, DBTTF−TCNQ, and STB−F_4TCNQ crystals. The spectra are obtained through expanding the E_{pol} and L values for the individual normal modes with Gaussian distribution functions; the full width at half-maximum (fwhm) is set to 20 cm^{-1}.

planar conformation, the contribution from low-frequency modes to the polaron binding energy is also negligible for holes. The computed E_{pol} values for holes (based on planar geometry for the neutral states) are about 140, 125, and 146 meV for STB, DBTTF, and DMQtT, respectively; for the sake of comparison, the respective values in pentacene[44] and rubrene[35] are equal to 49 and 80 meV, correspondingly. Thus, in the solid state, the local electron−phonon interactions for both electrons and holes are essentially similar in all three crystals.

We turn now to the discussion of the nonlocal electron−phonon coupling mechanism. In general, this mechanism has been much less studied than its local counterpart, and detailed quantum-chemical investigations of the nonlocal electron−phonon interactions have been performed only for a limited set of molecular crystals.[36,46] We have shown earlier that the overall strength of the nonlocal electron−phonon coupling can be quantified by a parameter (denoted here as L) that has the same physical meaning as E_{pol} in the case of local coupling. In the high-temperature limit where vibrations can be treated classically, parameter L defines the variance of the transfer integrals due to thermal fluctuations: $\sigma^2 = \langle(t - \langle t \rangle)^2\rangle = 2Lk_BT$. Here, $\langle \cdots \rangle$ represents the thermal average over the vibration manifold, k_B denotes the Boltzmann constant, and T is the temperature.

In the framework of the linear electron−vibration approximation, the transfer integral between neighboring sites has the following general dependence on the vibrational modes: $t_{i,i+1} = t^{(0)}_{i,i+1} + \sum_n[v^s_n(u_{ni} + u_{n,i+1}) + v^a_n(u_{ni} - u_{n,i+1})]$. Here, u_{ni} represents the nth vibration coordinates associated with site i; the first term is the transfer integral at the equilibrium crystal geometry, while the last two terms refer to the symmetric and antisymmetric nonlocal coupling mechanisms, respectively.[47] In the case of antisymmetric coupling, the change in a vibration coordinate u_{ni} results in an increase in the transfer integral between molecule i and its neighbor on one side and a decrease in the transfer integral with its neighbor on the other side. In the case of symmetric coupling, both transfer integrals vary in the same way. The description of the nonlocal interactions in CT crystals due to the superexchange nature of the electronic coupling represents a very complex problem, and a complete discussion of this mechanism will be provided elsewhere. In order to estimate the electron−vibration couplings along the molecular stacks, we have used here a simplified approach based on the eq 2 (see the Supporting Information).

The results of our calculations, see Figure 4, reveal that, in the present CT systems, a given vibration contributes only to either symmetric or antisymmetric coupling. As in the case of the transfer integrals, the nonlocal couplings for holes and electrons are very similar. As seen from Figure 4, the nonlocal coupling is much stronger for antisymmetric vibrations than for symmetric vibrations. For instance, the contributions to the relaxation energy for holes in DMQtT−F_4TCNQ are about 2.74 and 11.76 meV for the symmetric and antisymmetric coupling (L_s and L_a), respectively. The calculations also show that the relaxation energies due to both mechanisms are dominated by the contributions from low-frequency (in general, intermolecular) vibrations. The estimated standard deviations at room temperature due to the overall effect of all modes are about four times as small as the values of the respective transfer integrals. Thus, the calculations indicate that the nonlocal electron−phonon couplings are modest.

3.3. Charge-Transport Properties. Finally, we estimated the carrier mobilities along the stacking direction by employing a semiclassical one-dimensional model. The following one-dimensional two-mode Hamiltonian has been used:

$$H = H_{el} + H_L \tag{3}$$

$$H_{el} = \sum_i [t^{(0)} + v^s(u^s_i + u^s_{i+1}) + v^a(u^a_i - u^a_{i+1})] (c^+_{i+1}c_i + c^+_i c_{i+1}) \tag{4}$$

$$H_L = \sum_i \frac{\hbar\omega_s}{2}[(p^s_i)^2 + (u^s_i)^2] + \sum_i \frac{\hbar\omega_a}{2}[(p^a_i)^2 + (u^a_i)^2] \tag{5}$$

Here, ω_s and ω_a are the frequencies of symmetric and asymmetric vibrations, respectively. In this model, only the nonlocal interactions are explicitly included, and the interactions are reduced to one effective symmetric mode and one antisymmetric mode. In the spirit of small polaron theory,[40] we assume here that the role of local electron−phonon interactions[48] is to renormalize the electronic couplings. Therefore, in order to account for the interactions with high-frequency vibrations contributing to the local coupling mechanism, the transfer integral and nonlocal coupling constants in eq 4 have been modified according to[40]

$$t \rightarrow t \exp\{-E_{pol} \coth(\hbar\omega_i/2k_BT)/\hbar\omega_i\} \tag{6}$$

$$v \rightarrow v \exp\{-E_{pol} \coth(\hbar\omega_i/2k_BT)/\hbar\omega_i\} \tag{7}$$

dx.doi.org/10.1021/ja210284s | J. Am. Chem.Soc. 2012, 134, 2340−2347

In these formulas, ω_i is the frequency of an effective high-frequency mode. Based on the derived electron−phonon coupling constants (see Figure 4), we used in our calculations the following values for the effective vibration frequencies (a moderate change in these has no effect on the derived conclusions): ω_i = 1200 cm^{-1} and $\omega_s = \omega_a$ = 60 cm^{-1}.

The mobilities were calculated by a mixed quantum-classical dynamics method applied recently to single-component organic semiconductors[49] (the details of the methodology are thoroughly described in the Supporting Information). The calculated mobilities and their temperature dependence are shown in Figure 5. The mobilities show a power-law

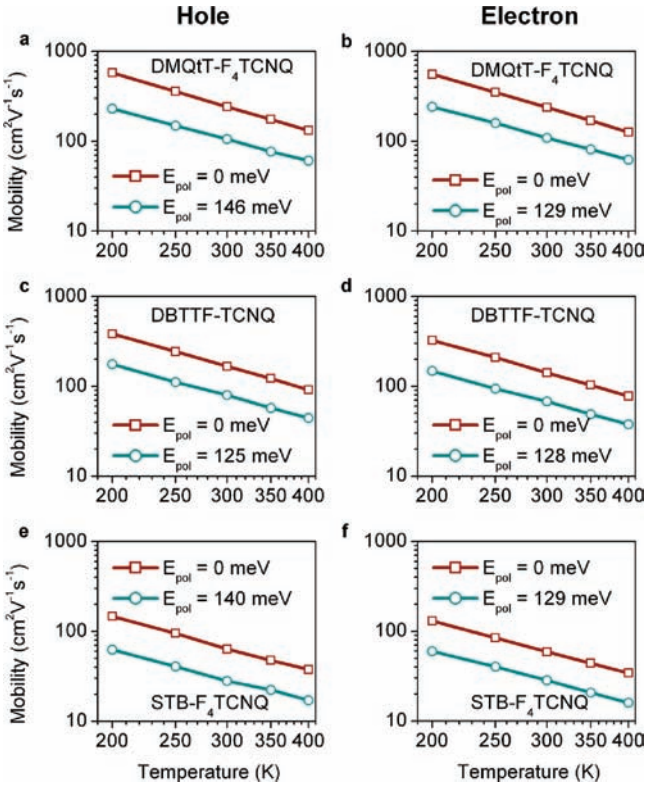

Figure 5. Temperature dependence of the hole and electron mobilities along the stacking directions. The mobilities were calculated with (circle) and without (square) accounting for the local electron−phonon interaction (renormalization of the transfer integrals).

dependence on temperature, which suggests bandlike transport in all systems. The mobilities are very large, ranging at room temperature from about 30 cm^2/(V s) in STB−F_4TCNQ to about 100 cm^2/(V s) in DMQtT−F_4TCNQ. As expected from our earlier discussion, the mobilities for holes and electrons are comparable. The largest difference is obtained for DBTTF−TCNQ where the calculated room-temperature mobilities for electrons and holes along the stacking direction are 68 and 80 cm^2/(V s), respectively.

We note that the mobility calculated for DBTTF−TCNQ is significantly larger than the overall value of 1 cm^2/(V s) for electrons derived from FET measurements.[15] This discrepancy has two likely sources. First, our calculations do not account for the interactions with acoustic vibrations and intermolecular contribution to the local coupling mechanism; as a result, the calculated values are expected to be somewhat overestimated. On the other hand, on the experimental side, it is well-known that the FET mobility can be significantly reduced due to interaction with the substrate, purity of the sample, and other factors.[50] Thus, the maximum value of the intrinsic mobility in this system is likely to be between the current experimental and computed values. In addition, our calculations suggest that the hole mobility should be slightly larger than the electron mobility.

4. CONCLUSIONS

To summarize, we have investigated the electronic structure and charge-transport properties of three CT crystals: DBTTF−TCNQ, DMQtT−F_4TCNQ, and STB−F_4TCNQ. Very large transfer integrals (small effective masses) and modest electron−phonon couplings are calculated for both holes and electrons. As a consequence, remarkable ambipolar charge-transport properties are predicted for all three crystals. In conclusion, our results provide strong theoretical support to recent suggestions in the literature that CT materials could represent a class of systems with high potential in organic electronics. Our results should stimulate for further experimental work to establish whether mobilities at room temperature in CT crystals can indeed rival or even surpass those in the best single-component organic crystals.

■ ASSOCIATED CONTENT

Supporting Information

Methodologies regarding the computations of transfer integrals, nonlocal coupling constants, and mobility parameters; valence and conduction total bandwidths and related bandwidths along the stacking directions; B3LYP/6-31G(d,p) and ωB97x/6-31G(d,p) results for the effective hole- and electron-transfer integrals; B3LYP and BHandHLYP results for band structures and hole and electron effective masses; symmetric and antisymmetric components of parameter L; spectra of nonlocal electron−vibration couplings for symmetric and antisymmetric normal modes; total energies and unit-cell atomic coordinates of all optimized crystal structures; complete ref 30. This material is available free of charge via the Internet at http://pubs.acs.org.

■ AUTHOR INFORMATION

Corresponding Author

coropceanu@gatech.edu; jean-luc.bredas@chemistry.gatech.edu

Present Address

[†]Department of Polymer Science and Engineering, Dankook University, Jukjeon, Gyeonggi 448-701, Korea.

Notes

[‡]Also affiliated with the Department of Chemistry, King Abdulaziz University, Jeddah 21589, Saudi Arabia.

■ ACKNOWLEDGMENTS

This work has been funded in part by Solvay and by the National Science Foundation under Award No. DMR-0819885 of the MRSEC Program and Award No. DMR-1105147. We gratefully acknowledge computing resources in the School of Chemistry and Biochemistry at the Georgia Institute of Technology made available by the National Science Foundation under Award No. CHE-0946869 of the CRIF Program.

■ REFERENCES

(1) Greenham, N. C.; Moratti, S. C.; Bradley, D. D. C.; Friend, R. H.; Holmes, A. B. *Nature* **1993**, *365*, 628.
(2) Anthony, J. E. *Angew. Chem., Int. Ed.* **2008**, *47*, 452.

(3) Horiuchi, S.; Hasegawa, T.; Tokura, Y. *J. Phys. Soc. Jpn.* **2006**, *75*, 051016.
(4) Hasegawa, T.; Takeya, J. *Sci. Technol. Adv. Mater.* **2009**, *10*, 16.
(5) Mori, T.; Kawamoto, T. *Annu. Rep. Prog. Chem., Sect. C: Phys. Chem.* **2007**, *103*, 134.
(6) Ferraris, J. P.; Poehler, T. O.; Bloch, A. N.; Cowan, D. O. *Tetrahedron Lett.* **1973**, 2553.
(7) Coleman, L. B.; Cohen, M. J.; Sandman, D. J.; G., Y. F.; Garito, A. F.; Heeger, A. J. *Solid State Commun.* **1973**, *12*, 1125.
(8) Jerome, D.; Mazaud, A.; Ribault, M.; Bechgaard, K. *J. Phys. Lett.* **1980**, *41*, L95.
(9) Jerome, D. *Chem. Rev.* **2004**, *104*, 5565.
(10) Mori, T. *Chem. Rev.* **2004**, *104*, 4947.
(11) Mori, T. *J. Phys.: Condens. Matter* **2008**, *20*, 184010.
(12) Hasegawa, T.; Mattenberger, K.; Takeya, J.; Batlogg, B. *Phys. Rev. B* **2004**, *69*, 245115.
(13) Sakai, M.; Sakuma, H.; Ito, Y.; Saito, A.; Nakamura, M.; Kudo, K. *Phys. Rev. B* **2007**, *76*, 045111.
(14) Takahashi, Y.; Hasegawa, T.; Abe, Y.; Tokura, Y.; Nishimura, K.; Saito, G. *Appl. Phys. Lett.* **2005**, *86*, 063504.
(15) Takahashi, Y.; Hasegawa, T.; Abe, Y.; Tokura, Y.; Saito, G. *Appl. Phys. Lett.* **2006**, *88*, 073504.
(16) Pope, M.; Swenberg, C. E. *Electronic processes in organic crystals and polymers*, 2nd ed.; Oxford University Press: New York, 1999.
(17) Sing, M.; Schwingenschlogl, U.; Claessen, R. *Phys. Rev. B* **2003**, *68*, 125111.
(18) Ishibashi, S.; Kohyama, M. *Phys. Rev. B* **2000**, *62*, 7839.
(19) Alves, H.; Molinari, A. S.; Xie, H.; Morpurgo, A. F. *Nat. Mater.* **2008**, *7*, 574.
(20) Williams, R. S.; Wallwork, S. C. *Acta Crystallogr., Sect. B: Struct. Sci.* **1968**, *24*, 168.
(21) Shaanan, B.; Shmueli, U.; Rabinovich, D. *Acta Crystallogr., Sect. B: Struct. Sci.* **1976**, *32*, 2574.
(22) Shokaryev, I.; Buurma, A. J. C.; Jurchescu, O. D.; Uijttewaal, M. A.; de Wijs, G. A.; Palstra, T. T. M.; de Groo, R. A. *J. Phys. Chem. A* **2008**, *112*, 2497.
(23) Buurma, A. J. C.; Jurchescu, O. D.; Shokaryev, I.; Baas, J.; Meetsma, A.; de Wijs, G. A.; de Groot, R. A.; Palstra, T. T. M. *J. Phys. Chem. C* **2007**, *111*, 3486.
(24) Tickle, I. J.; Prout, C. K. *J. Chem. Soc., Perkin Trans. 2* **1973**, 720.
(25) Torrance, J. B.; Mayerle, J. J.; Bechgaard, K.; Silverman, B. D.; Tomkiewicz, Y. *Phys. Rev. B* **1980**, *22*, 4960.
(26) Kobayashi, H.; Nakayama, J. *Bull. Chem. Soc. Jpn.* **1981**, *54*, 2408.
(27) Emge, T. J.; Wiygul, F. M.; Chappell, J. S.; Bloch, A. N.; Ferraris, J. P.; Cowan, D. O.; Kistenmacher, T. J. *Mol. Cryst. Liq. Cryst.* **1982**, *87*, 137.
(28) Saunders, V. R.; Dovesi, R.; Roetti, C.; Orlando, R.; Zicovich-Wilson, C. M.; Harrison, N. M.; Doll, K.; Civalleri, B.; Bush, I. J.; D'Arco, P.; Llunell, M. *CRYSTAL06 User's Manual*; Torino, Italy, 2006.
(29) Valeev, E. F.; Coropceanu, V.; da Silva Filho, D. A.; Salman, S.; Brédas, J.-L. *J. Am. Chem. Soc.* **2006**, *128*, 9882.
(30) Frisch, M. J.;et al. *Gaussian 03*, revision E.01; Gaussian, Inc.: Wallingford, CT, 2004.
(31) Hotta, S.; Kobayashi, H. *Synth. Met.* **1994**, *66*, 117.
(32) Sato, A.; Okada, M.; Saito, K.; Sorai, M. *Acta Crystallogr., Sect. C: Cryst. Struct. Commun.* **2001**, *57*, 564.
(33) Hummer, K.; Ambrosch-Draxl, C. *Phys. Rev. B* **2005**, *72*, 205205.
(34) Coropceanu, V.; Cornil, J.; da Silva Filho, D. A.; Olivier, Y.; Silbey, R.; Brédas, J. L. *Chem. Rev.* **2007**, *107*, 926.
(35) da Silva Filho, D. A.; Kim, E.-G.; Brédas, J. L. *Adv. Mater.* **2005**, *17*, 1072.
(36) Sanchez-Carrera, R. S.; Paramonov, P.; Day, G. M.; Coropceanu, V.; Brédas, J. L. *J. Am. Chem. Soc.* **2010**, *132*, 14437.
(37) de Wijs, G. A.; Mattheus, C. C.; de Groot, R. A.; Palstra, T. T. M. *Synth. Met.* **2003**, *139*, 109.
(38) Li, Z. Q.; Podzorov, V.; Sai, N.; Martin, M. C.; Gershenson, M. E.; Di Ventra, M.; Basov, D. N. *Phys. Rev. Lett.* **2007**, *99*, 016403.
(39) Holstein, T. *Ann. Phys.* **1959**, *8*, 325.
(40) Holstein, T. *Ann. Phys.* **1959**, *8*, 343.
(41) Peierls, R. E. *Quantum Theory of Solids*; Oxford University Press: New York, 2001.
(42) Brovchenko, I. V. *Chem. Phys. Lett.* **1997**, *278*, 355.
(43) Martinelli, N. G.; Ide, J.; Sanchez-Carrera, R. S.; Coropceanu, V.; Brédas, J.-L.; Ducasse, L.; Castet, F.; Cornil, J.; Beljonne, D. *J. Phys. Chem. C* **2010**, *114*, 20678.
(44) Coropceanu, V.; Malagoli, M.; da Silva Filho, D. A.; Gruhn, N. E.; Bill, T. G.; Brédas, J. L. *Phys. Rev. Lett.* **2002**, *89*, 275503.
(45) Zhu, L. Y.; Kim, E.-G.; Yi, Y.; Ahmed, E.; Jenekhe, S. A.; Coropceanu, V.; Brédas, J. L. *J. Phys. Chem. C* **2010**, *114*, 20401.
(46) Coropceanu, V.; Sánchez-Carrera, R. S.; Paramonov, P.; Day, G. M.; Brédas, J. L. *J. Phys. Chem. C* **2009**, *113*, 4679.
(47) Zhao, Y.; Brown, D. W.; Lindenberg, K. *J. Chem. Phys.* **1994**, *100*, 2335.
(48) In the case of local coupling, the charge carriers interact most strongly with high-energy vibration modes; therefore, these interactions cannot be treated in the framework of a semiclassical approximation.
(49) Troisi, A.; Orlandi, G. *Phys. Rev. Lett.* **2006**, *96*, 086601.
(50) Hulea, I. N.; Fratini, S.; Xie, H.; Mulder, C. L.; Iossad, N. N.; Rastelli, G.; Ciuchi, S.; Morpurgo, A. F. *Nat. Mater.* **2006**, *5*, 982.